USGS
science for a changing world

Prepared in cooperation and collaboration with U.S. Fish and Wildlife Service via Gulf Coast Joint Venture, Texas A&M University-Kingsville, University of Louisiana-Lafayette, and Ducks Unlimited, Inc.

Delineation of Marsh Types of the Texas Coast from Corpus Christi Bay to the Sabine River in 2010

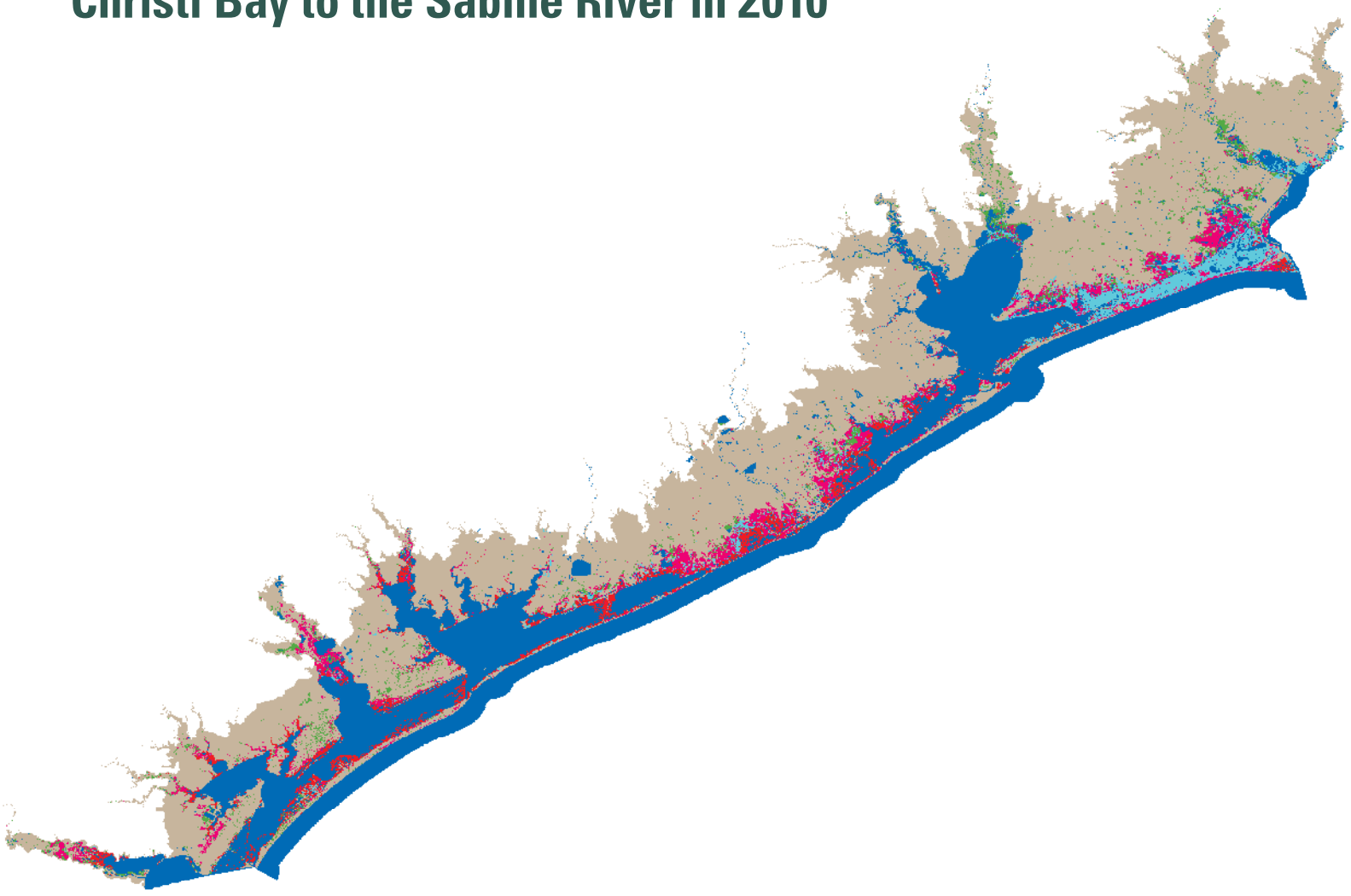

Scientific Investigations Report 2014–5110

U.S. Department of the Interior
U.S. Geological Survey

Delineation of Marsh Types of the Texas Coast from Corpus Christi Bay to the Sabine River in 2010

By Nicholas M. Enwright, Stephen B. Hartley, Michael G. Brasher, Jenneke M. Visser, Michael K. Mitchell, Bart M. Ballard, Mark W. Parr, Brady R. Couvillion, and Barry C. Wilson

Prepared in cooperation and collaboration with U.S. Fish and Wildlife Service via Gulf Coast Joint Venture, Texas A&M University-Kingsville, University of Louisiana-Lafayette, and Ducks Unlimited, Inc.

Scientific Investigations Report 2014–5110

U.S. Department of the Interior
U.S. Geological Survey

U.S. Department of the Interior
SALLY JEWELL, Secretary

U.S. Geological Survey
Suzette M. Kimball, Acting Director

U.S. Geological Survey, Reston, Virginia: 2014

Suggested citation:
Enwright, N.M., Hartley, S.B., Brasher, M.G., Visser, J.M., Mitchell, M.K., Ballard, B.M., Parr, M.W., Couvillion, B.R., and Wilson, B.C., 2014, Delineation of marsh types of the Texas coast from Corpus Christi Bay to the Sabine River in 2010: U.S. Geological Survey Scientific Investigations Report 2014–5110, 18 p., 1 pl., scale 1:400,000, *http://dx.doi.org/10.3133/sir20145110.*

ISSN 2328-0328 (online)

Acknowledgments

Funding for this work was provided by the U.S. Geological Survey South Central Climate Science Center, the U.S. Fish and Wildlife Service via the Gulf Coast Joint Venture, and Texas A&M University-Kingsville. We thank William Vermillion and Steve DeMaso of the Gulf Coast Joint Venture, Duane German of Texas Parks and Wildlife Department, David Diamond and Lee Elliott of the Missouri Resource Assessment Partnership, and Hailey Rue of the University of Louisiana-Lafayette for their assistance with the project and Joseph Spruce (National Aeronautics and Space Administration Stennis Space Center) and Steven Sesnie (U.S. Fish and Wildlife Service) for reviewing this work.

Contents

Figures

Tables

Conversion Factors

SI to Inch/Pound

Multiply	By	To obtain
	Length	
centimeter (cm)	0.3937	inch (in.)
meter (m)	3.281	foot (ft)
kilometer (km)	0.6214	mile (mi)
kilometer (km)	0.5400	mile, nautical (nmi)
meter (m)	1.094	yard (yd)
	Area	
square meter (m^2)	0.0002471	acre
hectare (ha)	2.471	acre
square hectometer (hm^2)	2.471	acre
square kilometer (km^2)	247.1	acre
square meter (m^2)	10.76	square foot (ft^2)
square kilometer (km^2)	0.3861	square mile (mi^2)
	Volume	
cubic hectometer (hm^3)	810.7	acre-foot (acre-ft)

Vertical coordinate information is referenced to the North American Vertical Datum of 1988 (NAVD 88) unless otherwise noted.

Horizontal coordinate information is referenced to the World Geodetic System 1984 (WGS 84) Universal Transverse Mercator (UTM) Zone 15 North.

Delineation of Marsh Types of the Texas Coast from Corpus Christi Bay to the Sabine River in 2010

By Nicholas M. Enwright, Stephen B. Hartley, Michael G. Brasher, Jenneke M. Visser, Michael K. Mitchell, Bart M. Ballard, Mark W. Parr, Brady R. Couvillion, and Barry C. Wilson

Abstract

Coastal zone managers and researchers often require detailed information regarding emergent marsh vegetation types for modeling habitat capacities and needs of marsh-reliant wildlife (such as waterfowl and alligator). Detailed information on the extent and distribution of marsh vegetation zones throughout the Texas coast has been historically unavailable. In response, the U.S. Geological Survey, in cooperation and collaboration with the U.S. Fish and Wildlife Service via the Gulf Coast Joint Venture, Texas A&M University-Kingsville, the University of Louisiana-Lafayette, and Ducks Unlimited, Inc., has produced a classification of marsh vegetation types along the middle and upper Texas coast from Corpus Christi Bay to the Sabine River. This study incorporates approximately 1,000 ground reference locations collected via helicopter surveys in coastal marsh areas and about 2,000 supplemental locations from fresh marsh, water, and "other" (that is, nonmarsh) areas. About two-thirds of these data were used for training, and about one-third were used for assessing accuracy. Decision-tree analyses using Rulequest See5 were used to classify emergent marsh vegetation types by using these data, multitemporal satellite-based multispectral imagery from 2009 to 2011, a bare-earth digital elevation model (DEM) based on airborne light detection and ranging (lidar), alternative contemporary land cover classifications, and other spatially explicit variables believed to be important for delineating the extent and distribution of marsh vegetation communities. Image objects were generated from segmentation of high-resolution airborne imagery acquired in 2010 and were used to refine the classification. The classification is dated 2010 because the year is both the midpoint of the multitemporal satellite-based imagery (2009–11) classified and the date of the high-resolution airborne imagery that was used to develop image objects. Overall accuracy corrected for bias (accuracy estimate incorporates true marginal proportions) was 91 percent (95 percent confidence interval [CI]: 89.2–92.8), with a kappa statistic of 0.79 (95 percent CI: 0.77–0.81). The classification performed best for saline marsh (user's accuracy 81.5 percent; producer's accuracy corrected for bias 62.9 percent) but showed a lesser ability to discriminate intermediate marsh (user's accuracy 47.7 percent; producer's accuracy corrected for bias 49.5 percent). Because of confusion in intermediate and brackish marsh classes, an alternative classification containing only three marsh types was created in which intermediate and brackish marshes were combined into a single class. Image objects were reattributed by using this alternative three-marsh-type classification. Overall accuracy, corrected for bias, of this more general classification was 92.4 percent (95 percent CI: 90.7–94.2), and the kappa statistic was 0.83 (95 percent CI: 0.81–0.85). Mean user's accuracy for marshes within the four-marsh-type and three-marsh-type classifications was 65.4 percent and 75.6 percent, respectively, whereas mean producer's accuracy was 56.7 percent and 65.1 percent, respectively.

This study provides a more objective and repeatable method for classifying marsh types of the middle and upper Texas coast at an extent and greater level of detail than previously available for the study area. The seamless classification produced through this work is now available to help State agencies (such as the Texas Parks and Wildlife Department) and landscape-scale conservation partnerships (such as the Gulf Coast Prairie Landscape Conservation Cooperative and the Gulf Coast Joint Venture) to develop and (or) refine conservation plans targeting priority natural resources. Moreover, these data may improve projections of landscape change and serve as a baseline for monitoring future changes resulting from chronic and episodic stressors.

Introduction

Detailed information on the extent and distribution of marsh vegetation zones throughout the Texas coast has been historically unavailable. Along the middle and upper Gulf of Mexico coast, broad-scale mapping and monitoring of coastal marsh vegetation zones have typically been conducted only in Louisiana (Chabreck and others, 1968; Chabreck and Linscombe, 1978, 1988, 1997, 2001; Visser and others, 1998, 2000; Sasser and others, 2008, 2014). Most existing large-scale land cover classifications for coastal Texas

identified emergent marsh as either palustrine (less than [<] 0.5 parts per thousand [ppt] salinity) or estuarine (≥0.5 ppt salinity) (for example, National Oceanic and Atmospheric Administration [NOAA] Coastal Change Analysis Program [C-CAP] and National Wetlands Inventory [NWI]) or used the combined categories of fresh-intermediate and brackish-saline to identify marsh types (for example, Texas Ecological Classification Systems [TECS] developed by the Texas Parks and Wildlife Department [TPWD] and Missouri Resource Assessment Partnership).

To help meet these data needs, the U.S. Geological Survey, in cooperation and collaboration with the U.S. Fish and Wildlife Service via the Gulf Coast Joint Venture, Texas A&M University-Kingsville, the University of Louisiana-Lafayette, and Ducks Unlimited, Inc., has produced a seamless and standardized classification of marsh vegetation types indicative of salinity zones (fresh, intermediate, brackish, and saline zones as discussed by Nyman and Chabreck, 2012) for the middle- and upper Texas coast from Corpus Christi Bay to the Sabine River (Texas/Louisiana border). These efforts were part of a larger, multiyear project to classify emergent marsh vegetation types along the north-central Gulf of Mexico coast from Corpus Christi Bay, Texas, to Mobile Bay, Alabama.

Natural resource scientists require spatially precise and thematically accurate land cover classifications for describing, modeling, and monitoring coastal systems to reflect their true dynamics and complexities (Glick and others, 2013; Johnson and others, 2013). The objective of this study was to develop baseline conditions by using a repeatable method for classifying marsh vegetation types of the middle and upper Texas coast at an extent and level of detail similar to that currently available for Louisiana.

These data are needed to enable State agencies (such as the TPWD) and landscape-scale conservation partnerships (for example, Gulf Coast Prairie Landscape Conservation Cooperative [GCP LCC] and the Gulf Coast Joint Venture [GCJV]) to develop and (or) refine conservation plans targeting priority natural resources in a consistent manner across the northern Gulf Coast. Moreover, these data may be used to improve projections of landscape change and serve as a baseline from which such changes can be measured (Sasser and others, 2008, 2014).

Methodology

The study area covered approximately 21,853 square kilometers (km^2) of coastal Texas and nearshore environments from Corpus Christi Bay to the Sabine River (fig. 1). The inland extent of the study area was defined by the 10-meter (m) elevation contour line, which was created from U.S. Geological Survey National Elevation Dataset (NED) 1/3-arc-second (10-m) elevation data (referenced to the North American Vertical Datum of 1988 [NAVD 88]) accessed in July 2012. The rationale for using the 10-m contour was to allow for monitoring of inland marsh migration by using trend analysis of future classifications. The study area extended seaward 5–6 kilometers (km) from the shoreline and included barrier islands and nearshore waters. Corpus Christi Bay marked the southernmost boundary of the study area because the Laguna Madre region south of Corpus Christi Bay is dominated by hypersaline waters and nonvegetated tidal flats (that is, limited emergent marsh occurs south of Corpus Christi Bay) (Osland and others, in press). Two distinct regions are found within the study area. The Texas Chenier Plain is the area east of Galveston Bay to the Sabine River (fig. 1; Gosselink and others, 1979). The Texas Mid-Coast extends south from Galveston Bay to Corpus Christi Bay (fig. 1; Wilson and Esslinger, 2002). Average annual precipitation ranges from 81 to 91 centimeters (cm) near Corpus Christi to about 127 to 152 cm near the Sabine River (Prism Climate Group, 2012). In addition to increased rainfall, the Texas Chenier Plain contains beach ridges and stranded beach ridges (cheniers), which limit tidal exchange to a few narrow coastal inlets off the Sabine River (Visser and others, 2000). Coastal marsh in the Texas Chenier Plain occurs in relatively more extensive zonations than commonly found in the Texas Mid-Coast, where marsh tends to occur as a tidal fringe along estuaries and tidal creeks (Wilson and Esslinger, 2002).

Land cover was delineated within the study area into six discrete classes: (1) fresh marsh, (2) intermediate marsh, (3) brackish marsh, (4) saline marsh, (5) water, and (6) "other" (nonmarsh). To achieve consistency with other large-scale marsh classifications in the northern Gulf Coast (Sasser and others, 2008, 2014), marsh was classified by following the system of Chabreck and others (1968). Salinity and vegetation community relations in Texas coastal marsh were assumed to be similar to those found in Louisiana. Thus in the study area, fresh marsh salinity ranges from 0.1 to 3.4 ppt with an average of 1.0 ppt and is commonly dominated by maidencane (*Panicum hemitomon*), spikerushes (*Eleocharis* spp.), and alligator weed (*Alternanthera philoxeroides*) (O'Neil, 1949; Chabreck, 1972). Intermediate marsh salinity ranges from 0.5 to 8.3 ppt with an average of 3.3 ppt and is commonly dominated by gulf cordgrass (*Spartina spartinae*), marshhay cordgrass (*Spartina patens*), bulltongue (*Sagittaria lancifolia*), and coastal waterhyssop (*Bacopa monnieri*) (Chabreck, 1972; Nyman and Chabreck, 2012). Brackish marsh salinity ranges from 1.0 to 18.4 ppt with an average of 8.2 ppt and is typically dominated by marshhay cordgrass (*Spartina patens*) and seashore saltgrass (*Distichlis spicata*) (Chabreck, 1972; Nyman and Chabreck, 2012). Saline marsh salinity ranges from 8.1 to 29.4 ppt with an average of 18.0 ppt and is typically dominated by smooth cordgrass (*Spartina alterniflora*), seashore saltgrass (*Distichlis spicata*), and needlegrass rush (*Juncus roemerianus*) (Chabreck, 1972; Nyman and Chabreck, 2012).

Marsh vegetation types were classified by using classification decision-tree (DT) analyses and rulesets produced by using Rulequest See5 Release 2.09 (See5) in combination with ERDAS Imagine 2010, National Land

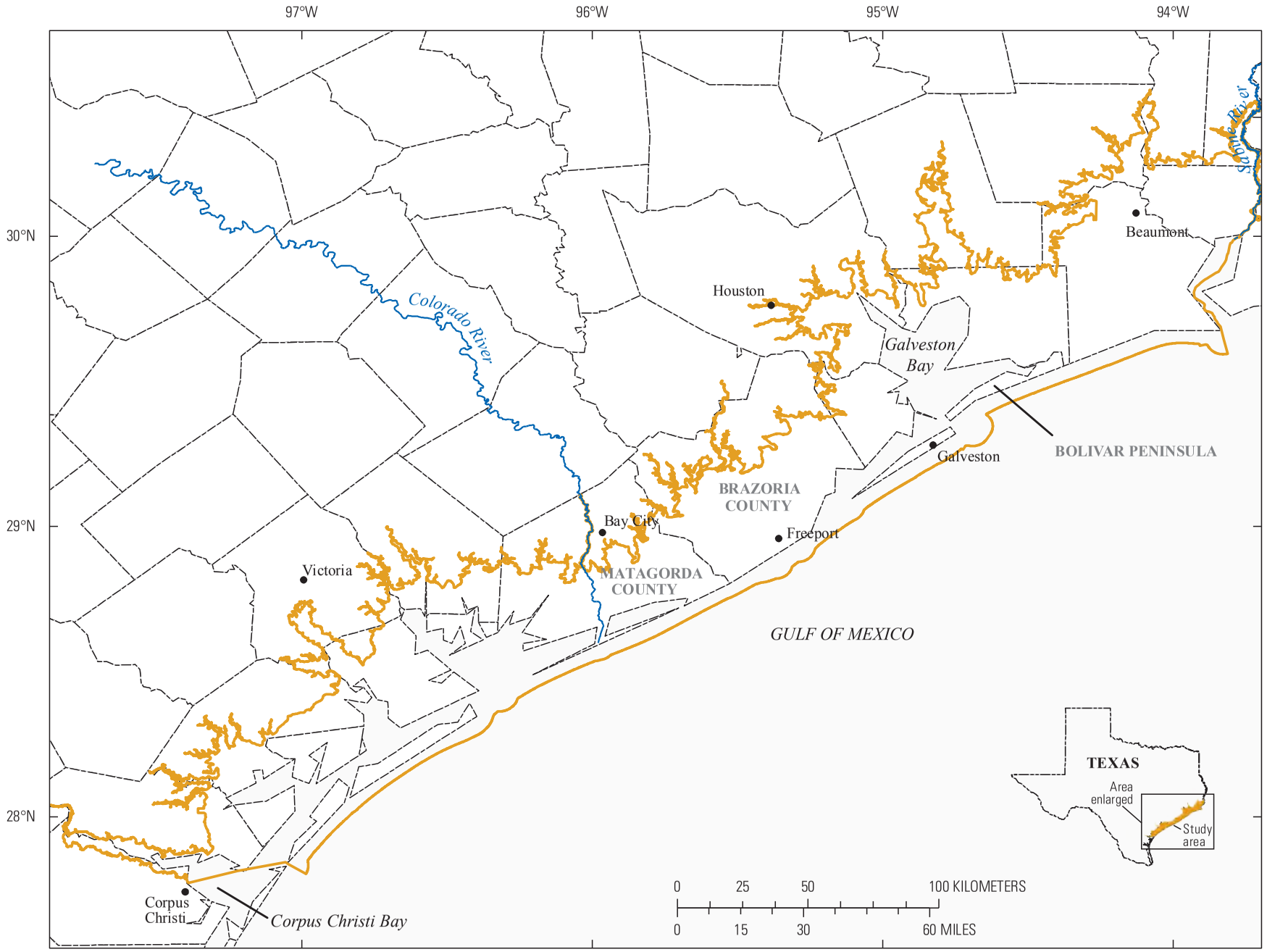

Figure 1. Study area, middle to upper Texas coast.

Cover Dataset (NLCD) Mapping Tool v2.087, ESRI ArcMap 10.1, and Trimble eCognition. See5 has been used to produce NLCD classifications (Homer and others, 2007), NOAA C-CAP land cover classifications, and a NOAA project that mapped the shallow-water benthic habitats in south Texas (Finkbeiner and others, 2009). DT analyses utilize a suite of independent spatial variables (predictor variables) and ground reference data (dependent variables) to develop multivariate decision trees for classifying a target area. Ground reference data used in this study included observations collected from helicopter surveys during October 2011 and October 2012 (Mitchell and others, in press), in-place observations by TPWD in 2009, and photoverification of ancillary datasets. Independent variables included multitemporal satellite-based imagery from 2009–2011, a bare-earth digital elevation model (DEM) based on airborne light detection and ranging (lidar), contemporary land cover classifications (C-CAP, TECS, and NWI), and proximity to the intertidal zone, with the upper boundary defined by the mean high higher water (MHHW) level.

The spatial resolution of this classification was set to 10 m. See5 and ERDAS Imagine require that all data have the same spatial resolution and registration when using DT analyses. Schmidt and others (2004) found elevation to be the greatest determining factor for mapping coastal vegetation by using an expert ruleset. Inundation frequency, a function of elevation, was found to influence marsh communities for marshes in coastal Louisiana (Couvillion and Beck, 2013); therefore, to best leverage high-resolution (3-m) airborne lidar bare-earth NED DEMs available in the study area, all datasets used in the DT analyses were resampled to 10 m from their native resolution.

Spectral variability within the study area was reduced by application of an exclusion mask identifying areas of urban and cultivated land cover types. The exclusion mask was created by combining the 2011 National Agriculture Statistics Service (NASS) Crop Mask (that is, cultivated; Boryan and others, 2011) and the 2006 C-CAP urbanized classes. Areas intersecting the mask were removed from the classified area and coded to "other."

Five Landsat Thematic Mapper (TM) scenes provided complete coverage of the study area (fig. 1). Classifications were generated separately for each Landsat TM scene. Scene-specific classifications were mosaicked to create a seamless classification of the study area. During the mosaicking process, scenes containing a greater proportion of the study region were used for the overlap area common to adjacent scenes; for example, Path 25 Row 39 was overlaid on Path 24 Row 39. Two exceptions, however, were made to alleviate several edge-matching issues, such as hard/unnatural transitions that sometimes occur as a result of a scene change, associated with mosaicking the Landsat TM scenes. In the first exception, parts of Bolivar Peninsula and the southeastern Galveston Bay shoreline were removed from Path 25 Row 40 and instead mapped from the classification of Path 25 Row 39. In the second exception, areas west of the Colorado River were removed from the Path 25 Row 40 and instead mapped from the classification of Path 26 Row 40.

The subsequent sections provide details on acquisition of reference data, selection of training and accuracy assessment data, independent variables, stepwise classification methods, and accuracy assessment.

Reference Data and Selection of Training and Accuracy Points

Ground reference data were collected during October 2011 and October 2012 by using helicopter-based surveys. Survey transects were oriented north-south and spaced at 2-km intervals across the study area. Sample locations for collecting reference data were established along transects in a systematic manner, with an approximate spacing of 0.25 km between each location; however, the spacing was varied between some locations to maximize the number of samples intersecting marsh in areas characterized by a relatively narrow marsh zone. In October 2011, ground reference data were collected from 339 sample locations in Matagorda and Brazoria Counties in the Texas Mid-Coast (Mitchell and others, in press). Ground reference data were collected during October 2012 from an additional 637 sample locations across the remainder of the study area. Data collection at reference locations followed protocols of Visser and others (1998, 2000) and involved hovering 10 m above the marsh surface and recording the plant species and their respective coverage within a 30-m radius of the reference location. Two-way indicator species analysis (TWINSPAN) was used to separate helicopter-based reference locations into four marsh vegetation classes (marsh types): fresh, intermediate, brackish, and saline. Locations that did not intersect marsh were recorded as either "water" or "other" on the basis of field observations.

Helicopter-based reference locations were supplemented with approximately 80 marsh vegetation observations that were previously used as ground reference data for the TECS land cover classification. Because of the limited distribution of fresh marsh within the study area, few reference data for fresh marsh were collected during the helicopter survey. Two Landsat TM scenes did not contain any fresh marsh reference locations, and the other three had less than 10 fresh marsh reference locations. Fresh marsh reference locations were supplemented with approximately 250 locations obtained from a random selection of palustrine emergent wetlands identified by NWI data. Supplemental locations were also added for the water and "other" classes. Approximately 700 supplemental reference locations were obtained for the water class by randomly generating sample locations within the water class of the 2006 C-CAP land cover classification. Approximately 1,000 supplemental reference locations for the "other" class were obtained by randomly generating locations outside areas identified as "wetland" in NWI data. All supplemental locations were verified via examination of 2010 National Agriculture Imagery Program (NAIP) color-infrared airborne

photography to ensure that areas with palustrine emergent marsh had not been converted to a different land cover and (or) land use. Refer to figure 2 for a breakdown of ground reference data points throughout the study area.

In some cases, ground reference locations and supplemental locations fell near the exclusion mask. Zonal statistics were used to compute the proportion of the area covered by the exclusion mask within a 30-m buffer of the center of the reference location. For each Landsat TM scene, ground reference location buffers without any exclusion mask were considered suitable for use in an accuracy assessment. Unmasked pixels from buffers that contained the exclusion mask were utilized as training data. This action ensured that all observations included in the accuracy assessment were areas that had been classified by using DT analyses and were not simply recoded as "other." For each class in each Landsat TM scene, approximately 30 percent of the suitable reference locations (those not containing any parts of the exclusion mask) were randomly selected for accuracy assessment. The remaining locations were used as training data in the DT analyses. Table 1 outlines the number of ground reference locations for each class in each Landsat TM scene and the number of those points utilized as training. Following the protocol of Visser and others (1998, 2000), reference locations (x,y coordinates) for training were buffered by 30 m and rasterized for use in DT analyses.

Independent Variables

Independent variables included multitemporal, multispectral-satellite imagery and indices, airborne lidar bare-earth DEMs, contemporary land cover classifications (C-CAP, TECS, and NWI), and proximity to the intertidal zone (table 2). All available cloud-free Landsat TM 5, SPOT 4, and SPOT 5 satellite imagery acquired between 2009 and 2011 were included to capture phenological differences, such as green-up and senescence periods, among coastal marsh plant species (table 3). SPOT 4 and (or) SPOT 5 imagery were used when cloud-free coverage acquired within a 30-day period were available for the entirety of a Landsat TM scene (table 3). Individual SPOT 4 and (or) SPOT 5 scenes were mosaicked to cover the Landsat TM scene of interest. Imagery was downloaded from the U.S. Geological Survey with the Standard Terrain Correction (Level 1T). Level 1T correction provides systematic radiometric and geometric accuracy by incorporating ground control points while employing a DEM for topographic accuracy. No further geometric correction was applied, except for subpixel shifts to ensure pixel alignment. All satellite multispectral imagery was processed in terms of top of atmosphere (TOA) reflectance units. The maximum extent of imagery for a particular Landsat TM scene (that is, for all dates) was determined. For each Landsat TM scene, imagery was clipped to the identified maximum extent, resampled to 10 m, and verified for registration. Additionally, the Modified Normalized Difference Water Index (MNDWI; Xu, 2006) and Normalized Difference Vegetation Index (NDVI; Rouse and others, 1974) were calculated and used as independent variables in the DT analyses. For all Landsat TM imagery, a tasseled cap transformation (Crist and Cicone, 1984) of Landsat TM bands 1–5 and 7 was applied to include brightness, greenness, and wetness indices as independent variables. Huang and others (2002) found that the brightness, greenness, and wetness of the derived transformation collectively explained over 97 percent of the spectral variation of individual scenes for a study based on 10 Landsat 7 Enhanced Thematic Mapper Plus (ETM+) representing a variety of landscapes in the United States in both leaf-on and leaf-off conditions.

Tidal influence and flooding frequency, both of which are related to elevation, are two critical factors affecting salinity levels and inundation-related plant stress, thus influencing vegetation communities in a marsh environment (Tiner, 1993). Lidar-based NED 1/9-arc-second data (3-m) DEMs were used for the majority of the study area, but NED 1/3-arc-second (10-m) DEMs were used for areas where NED 1/9-arc-second data were unavailable. To capture the potential influence of local tides, NOAA VDatum v3.1 was used to transform NED DEMs from a vertical datum of NAVD 88 to local mean sea level (LMSL; Parker and others, 2003; Xu and others, 2013). The output of VDatum v3.1 provides the necessary information to transform a DEM into a tidal datum for tidally influenced areas but not for areas farther inland. The vertical datum for inland areas was transformed into LMSL by extrapolating the mean relative difference between NAVD 88 and LMSL for wide transects extending inland along the coast. The Euclidean distance from the MHHW zone, obtained from NOAA (Marcy and others, 2011), was calculated and used as a proxy for the likelihood of an area being exposed to elevated salinity.

The steady state compound topographic index (CTI; Moore and others, 1991), which expresses the potential water flow to a particular point from upslope areas, was used to help delineate between uplands and wetlands. The CTI has been calculated by the U.S. Geological Survey Earth Resources Observation and Science (EROS) Center for the conterminous United States by using NED 1-arc-second elevation data (30 m; EROS, 2003). By using the same process, a CTI layer was generated from lidar-based DEMs used in this study (10 m) to help delineate between uplands and wetlands.

Several existing contemporary land cover classifications were modified for use as independent variables. NWI data were simplified into the following nine classes: (1) agriculture, (2) palustrine emergent marsh, (3) palustrine emergent marsh/scrub-shrub mix, (4) palustrine scrub-shrub, (5) palustrine forested, (6) estuarine emergent marsh, (7) estuarine scrub-shrub, (8) upland, and (9) water. The TECS data contain greater detail than does C-CAP; thus, TECS data were crosswalked by combining more detailed classes to the appropriate C-CAP classification scheme (for example, the Chenier Plain comprises saline and brackish low tidal

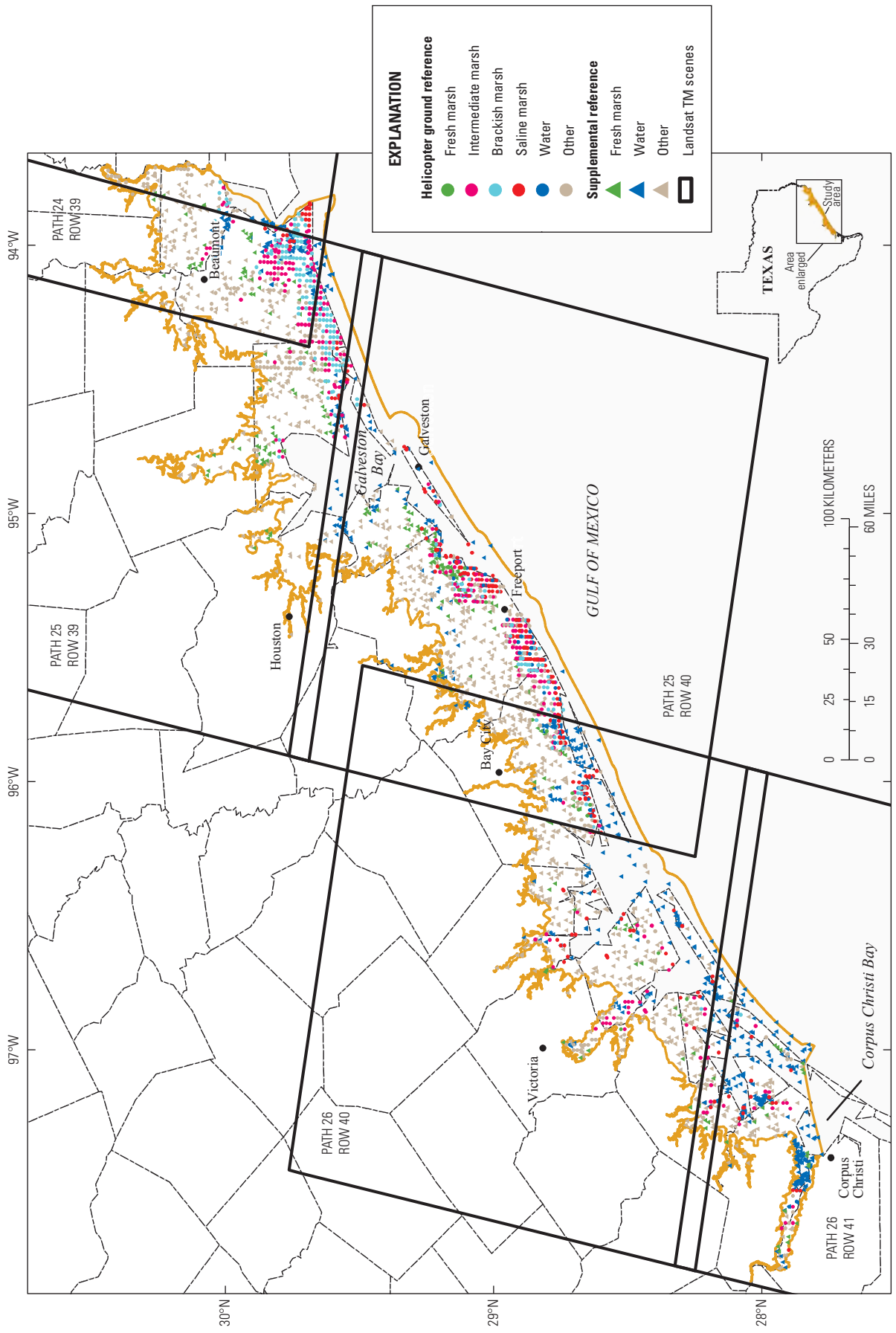

Figure 2. Study area, locations of ground reference data points, and spatial coverage of Landsat Thematic Mapper (TM) scenes, middle to upper Texas coast.

Table 1. Distribution of ground reference data and supplemental data among marsh and nonmarsh classes, middle to upper Texas coast, 2009–11.

[RL, number of total reference locations; RT, number of reference locations used for training; --, not applicable]

	Path 26 Row 41		Path 26 Row 40		Path 25 Row 40		Path 25 Row 39		Path 24 Row 39	
Class	**RL (original/ supplemental)**	**RT**	**RL (original/ supplemental)**	**RT**	**RL (original/ supplemental)**	**RT**	**RL (original/ supplemental)**	**RT**	**RL (original/ supplemental)**	**RT**
Fresh marsh	0/29	21	9/43	35	9/90	70	3/95	75	0/39	28
Intermediate marsh	27/--	17	58/--	35	124/--	81	127/--	90	89/--	63
Brackish marsh	4/--	3	22/--	13	87/--	57	133/--	96	90/--	63
Saline marsh	22/--	16	77/--	49	181/--	119	27/--	18	19/--	13
Water	2/272	188	20/191	132	48/134	111	0/106	66	0/100	72
Other	13/87	75	58/276	243	84/287	278	70/247	24	59/117	128

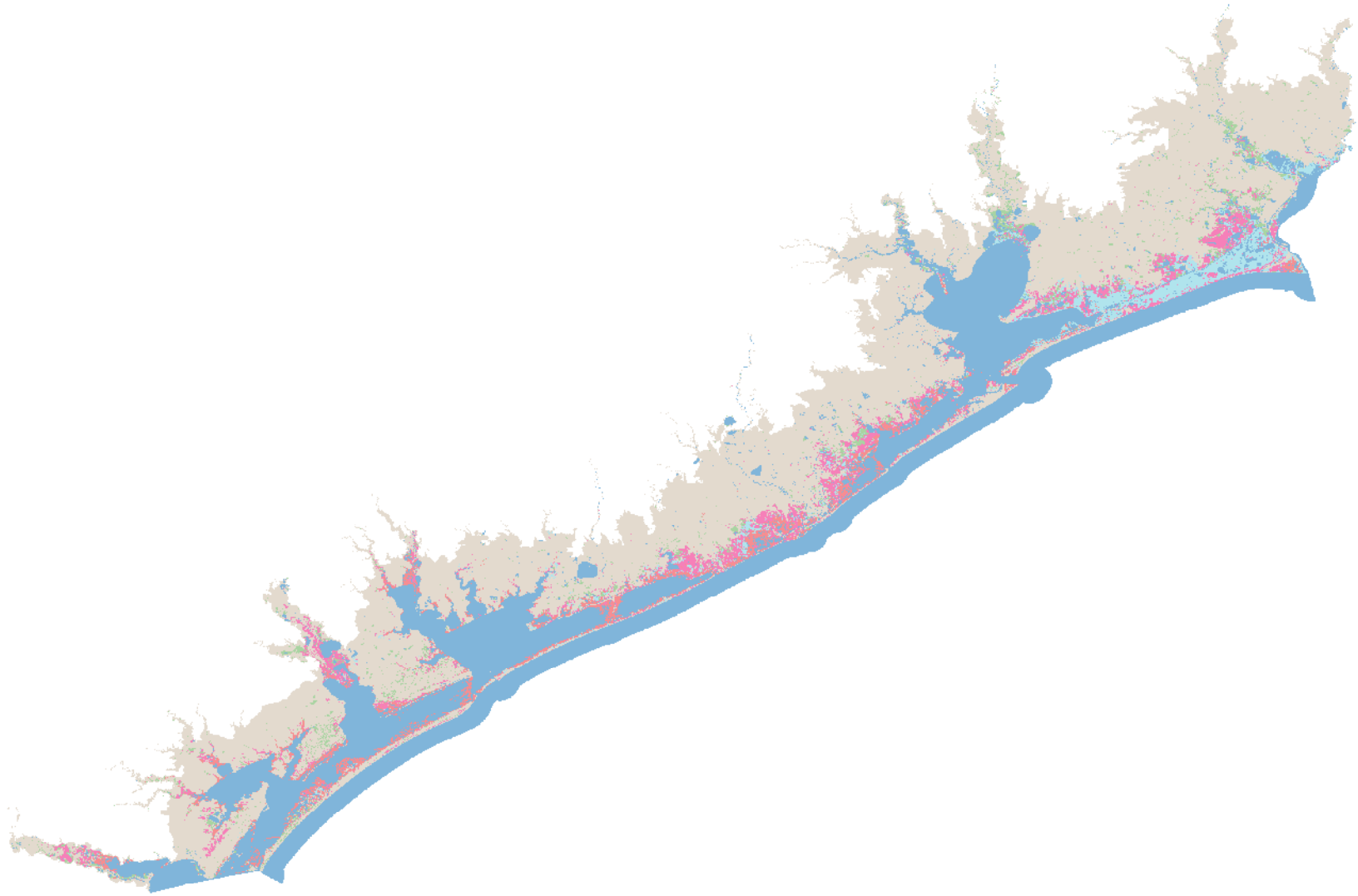

Table 2. Independent variables, source of data, and use for classification of marsh types along the middle to upper Texas coast, 2010.

	Independent variable	Source of data	Use
Spectral variables	Multitemporal, multispectral-satellite at-satellite reflectance	Landsat Thematic Mapper (TM); SPOT 4; SPOT 5	Discriminate spectral differences found in training data using decision-tree (DT) analyses.
	Modified Normalized Difference Water Index (MNDWI)	Landsat TM; SPOT 4; SPOT 5 (Xu, 2006)	Map land and (or) water by using thresholding; discriminate spectral differences found in training data by using DT analyses.
	Normalized Difference Vegetation Index (NDVI)	Landsat TM; SPOT 4; SPOT 5 (Rouse and others, 1974)	Discriminate spectral differences and phenology found in training data by using DT analyses.
	Tasseled cap transformation of Landsat TM imagery	Landsat TM (Crist and Cicone, 1984)	Brightness, greenness, and wetness bands were used to help discriminate spectral differences and phenology identified in training data by using DT analyses.
Topographic variables	Lidar-based National Elevation Dataset (NED) 1/9-arc-second data (3-m) digital elevation model (DEM) transformed to from North American Vertical Datum of 1988 (NAVD 88) to local mean sea level (LMSL)	U.S. Geological Survey NED and National Oceanic and Atmospheric Administration (NOAA) VDatum v3.1	Identify spatial patterns in topography of marsh vegetation types identified in training data by using DT analyses.
	Euclidean distance from the intertidal zone (mean high higher water [MHHW] zone)	Derived from the MHHW zone obtained from NOAA (Marcy and others, 2011)	Used as a proxy for the likelihood of an area being exposed to elevated salinity.
	Steady state compound topographic index (CTI)	Derived for this project using U.S. Geological Survey NED and CTI algorithm (Moore and others, 1991)	Delineate between uplands and wetlands.
Contemporary land cover	National Wetlands Inventory (NWI) simplified into the nine classes	U.S. Fish and Wildlife Service	Leverage existing classifications.
	NOAA Coastal-Change Assessment Program (C-CAP) land cover 2006	NOAA	Leverage existing classifications.
	Texas Ecological Classification System (TECS) crosswalked into the C-CAP classification system	Texas Parks and Wildlife Department and Missouri Resource Assessment Partnership	Leverage existing classifications.
	Sum of areas mapped as wetland in NWI, C-CAP, and TECS	Derived for this project	Delineate between uplands and wetlands.

Table 3. Satellite imagery acquisition dates by Landsat Thematic Mapper (TM) scenes, middle to upper Texas coast, 2009–11.

[--, not applicable]

Year	Path 26 Row 41	Path 26 Row 40	Path 25 Row 40	Path 25 Row 39	Path 24 Row 39
2009	11/01/2009	11/01/2009	05/18/2009	02/11/2009	01/19/2009
	--	--	11/10/2009	05/18/2009	02/04/2009
	--	--	--	11/26/2009	02/20/2009
	--	--	--	--	10/18/2009
	--	--	--	--	11/03/2009
	--	--	--	--	12/05/2009
2010	03/25/2010	03/28/2010	03/18/2010	03/18/2010	01/22/2010
	05/28/2010	05/28/2010	05/05/2010	05/5/2010	04/28/2010
	10/2010[1]	10/03/2010	--	08/25/2010	08/02/2010
	10/3/2010	12/06/2010	--	--	10/05/2010
	11/4/2010	--	--	--	11/06/2010
2011	10/2011[1]	10/2011[1]	08/28/2011	10/31/2011	06/02/2011
	--	--	10/31/2011	--	09/06/2011

[1]Mosaic of SPOT 4/5 imagery used for Landsat TM scene.

marsh and, thus, was coded to estuarine emergent marsh). The rationale for this process was to minimize introducing errors of contemporary classifications and place greater emphasis of the classification on spectral characteristics and elevation. Additionally, NWI, C-CAP, and TECS were simplified into a classification of upland (value of 1) or wetland (value of 2). These three layers were summed to identify agreement between the classifications (values ranging from 3 [upland in all three datasets] to 6 [wetland in all three datasets]).

Stepwise Classification Approach

The final classification was derived by using a stepwise classification approach from general to increasingly specific marsh classifications to reduce misclassification errors. Figure 3 outlines the stepwise process used in this study. This process was conducted separately for each Landsat TM scene. In the first step, each individual scene of imagery was classified into "land" and "water" by using an MNDWI threshold (Step 1). For each Landsat TM scene, all dates were then combined in ERDAS Imagine to create a majority land and (or) water map. Next, for each date, the land area identified in Step 1 was classified into "wetland," "water," and "other" by using DT analyses (Step 2). Water and "other" classes were included in this classification to possibly catch any errors of omission associated with Step 1. Independent variables for this step included (1) single date imagery and indices, (2) elevation data, (3) CTI, and (4) the sum of wetland and (or) upland data for NWI, C-CAP, and TECS. The maximum wetland area was mapped by combining the classifications developed in Step 2 for all dates of each Landsat TM scene. The expand function in ArcMap was used to expand this area by three pixels (30 m) to account for potential edge errors in wetland classification. Next, a single classification comprising all dates per Landsat TM scene of saline marsh, nonsaline marsh (fresh marsh, intermediate marsh, and brackish marsh), water, and "other" was conducted within the maximum extent of the wetland area identified in the previous step by using DT analyses (Step 3). (Again, "water" and "other" classes were included in this classification to possibly catch any errors of omission associated with Step 2). The nonsaline marsh pixels were then classified into "fresh," "intermediate," and "brackish" marsh (Step 4). Independent variables for Step 3 and Step 4 included (1) multitemporal imagery and indices, (2) elevation data, (3) Euclidean distance from intertidal zone, (4) C-CAP, (5) NWI, and (6) TECS. A series of overlays were used to combine the classifications into a preliminary classification depicting the extent of marsh vegetation zones (fresh, intermediate, brackish, and saline), upland, and "other" (Step 5). This process included overlaying the classification produced in Step 4, the majority water classification produced in Step 1, and the exclusion mask with all pixels in the mask being recoded to "other." Last, eCognition was used to generate image objects generated from 2010 NAIP color-infrared aerial photography (Step 6). The final classification was produced by using a script in ArcMap to determine the majority class for each image object.

Accuracy Assessment

To be consistent with methods used to develop ground reference data and to adhere to recommendations of Congalton and Green (2009) for using a cluster of pixels when assessing accuracy, we buffered the accuracy assessment locations by 30 m and determined the majority class for each. The error matrix for this classification is presented in table 4. Congalton and Green (2009) recommended 75–100 accuracy assessment points for each class to assess accuracy in study areas that

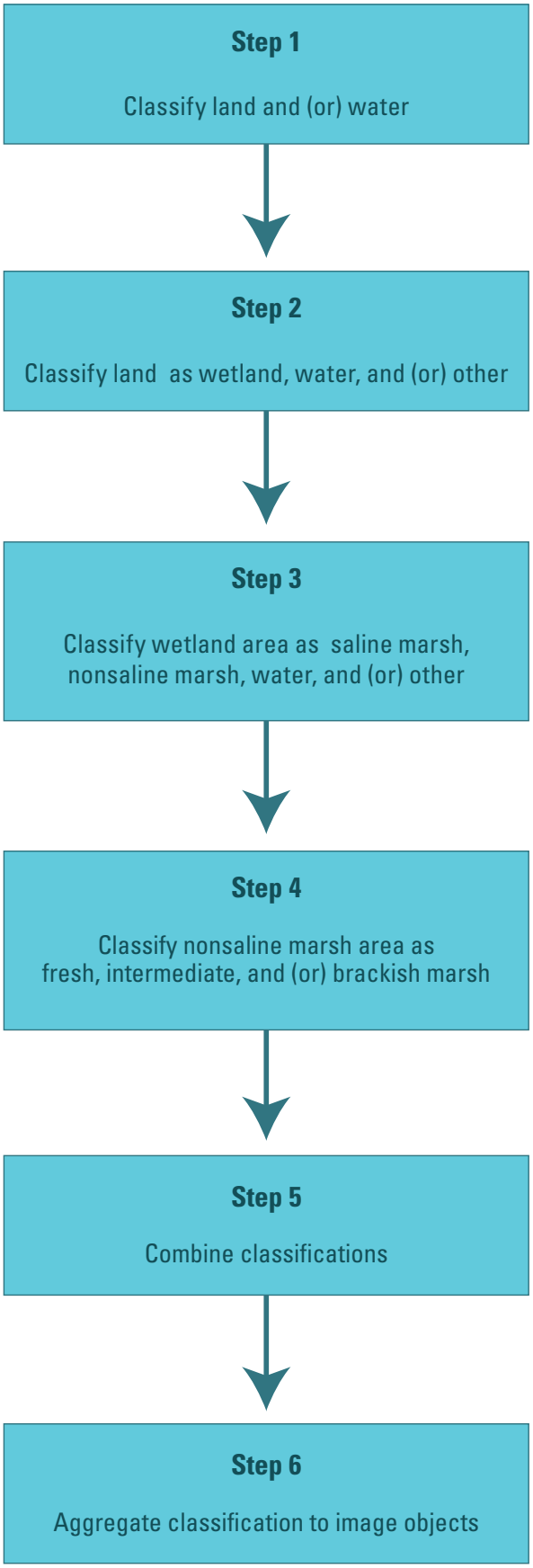

Figure 3. Conceptual model for stepwise classification process.

are considered large (greater than 4,047 km^2). Sample sizes for this study were sufficient to satisfy this recommendation for all classes except fresh marsh and brackish marsh, which had 65 accuracy assessment points each. Helicopter surveys were concentrated on wetland areas along the coast, resulting in a smaller number of reference locations for the water and "other" classes. Consequently, a greater number of accuracy points were added for water and "other" to reflect the large percentage of the study area composed of these classes (33 percent and 53 percent, respectively, of 21,907 km^2 mapped). Figure 4 shows the delineation of marsh vegetation types in coastal Texas.

The overall accuracy corrected for bias, which incorporated true marginal proportions (Congalton and Green, 2009) of the classification, was 91 percent (95 percent CI: 89.2–92.8), and the kappa statistic was 0.79 (95 percent CI: 0.77–0.81) (table 4). The agreement between classification and reference data was significantly greater than zero (z-statistic (Z) = 6.82, $p < 0.001$), indicating that the classification was better than that derived through random classification. As expected, water and "other" classes were mapped with a high degree of accuracy (about 95 percent user's and producer's accuracy for both classes); however, individual marsh types were less accurately classified. Of the four marsh types, saline marsh was classified with greatest accuracy; user's accuracy was 81.5 percent (95 percent CI: 78.7–84.3), and producer's accuracy corrected for bias was 62.9 percent (95 percent CI: 62.9–62.9). Intermediate marsh was classified with least accuracy, with a user's accuracy of 47.7 percent (95 percent CI: 44.1–51.3) and a producer's accuracy corrected for bias of 49.5 percent (95 percent CI: 43.9–55.1). Intermediate marsh was most readily confused with brackish marsh and fresh marsh. During the helicopter surveys, it was difficult to distinguish differences between the dominant plant species in these marshes. Marshhay cordgrass in the brackish marsh and gulf cordgrass in the intermediate marsh looked very similar from a distance and could only be distinguished when hovering above the station. For all marsh vegetation classes, mean user's accuracy was 65.4 percent, and mean producer's accuracy corrected for bias was 56.7 percent.

Because of the confusion with intermediate and brackish marsh, an alternative classification containing only three marsh types was created in which intermediate and brackish marsh were combined into a single class. This classification was generated by aggregation of the intermediate and brackish marsh pixels from the classification produced in Step 5 (fig. 3) and then by rerunning aggregation of classification to image objects (Step 6). This approach caused the areal coverage for each class to vary slightly between the four- and three-marsh-type classifications. As a result, these classifications should be considered separate products.

The overall accuracy corrected for bias for the alternative three-marsh-type classification (fig. 5) was 92.4 percent (95 percent CI: 90.7–94.2), and the kappa statistic was 0.83 (95 percent CI: 0.81–0.85) (table 4). Similar to the four-marsh-type classification, the agreement between the classification and reference data was significantly greater than zero ($Z = 7.22$, $p < 0.001$), indicating that the three-marsh-type

Table 4. Error matrices for four-marsh-type and three-marsh-type classifications, middle to upper Texas coast, 2010.

[FM, fresh marsh; IM, intermediate marsh; BM, brackish marsh; SM, saline marsh; W, water; O, other; CI, confidence interval]

Four-marsh-type classification

		Reference data							User's accuracy[1]	Square kilometers mapped
		FM	IM	BM	SM	W	O	Row total		
Map data	FM	**48**	8	2	0	1	7	66	72.7 ±3.2	609.5
	IM	8	**42**	13	6	4	15	88	47.7 ±3.6	1,031.3
	BM	4	16	**40**	3	1	3	67	59.7 ±3.5	677.7
	SM	1	3	6	**66**	4	1	81	81.5 ±2.8	723.3
	W	0	1	1	2	**204**	1	209	97.6 ±1.1	7,220.6
	O	3	5	2	3	1	**230**	244	94.5 ±1.7	11,644.6
	Column total	64	75	64	80	215	257	**755**		
Producer's accuracy[2]		62.3 ±12.2	49.5 ±5.6	52.1 ±4.4	62.9 ±0.0	98.6 ±0.5	97.1 ±0.7			

Overall accuracy[2]: 91 percent (95 percent CI: 89.2–92.8)

Kappa statistic: 0.79 (95 percent CI: 0.77–0.81)

Three-marsh-type classification

		Reference data						User's accuracy[1]	Square kilometers mapped
		FM	IM/BM	SM	W	O	Row total		
Map data	FM	**47**	11	0	1	7	66	71.2 ±3.2	573.4
	IM/BM	11	**115**	8	5	16	155	74.2 ±3.1	1,805.5
	SM	1	9	**66**	4	1	81	81.5 ±2.8	705
	W	0	2	1	**205**	1	209	98.1 ±1.0	7,193.1
	O	3	8	3	2	**228**	244	93.4 ±1.8	11,630
	Column total	62	145	78	217	253	**755**		
Producer's accuracy[2]		59.3 ±12.7	68.2 ±3.8	67.9 ±0.0	97.3 ±0.4	97.4 ±0.7			

Overall accuracy[2]: 92.4 percent (95 percent CI: 90.7–94.2)

Kappa statistic: 0.83 (95 percent CI: 0.81–0.85)

[1]±X.X represents confidence interval at 95 percent.

[2]Corrected for bias by using true map marginal proportions; ±X.X represents confidence interval at 95 percent.

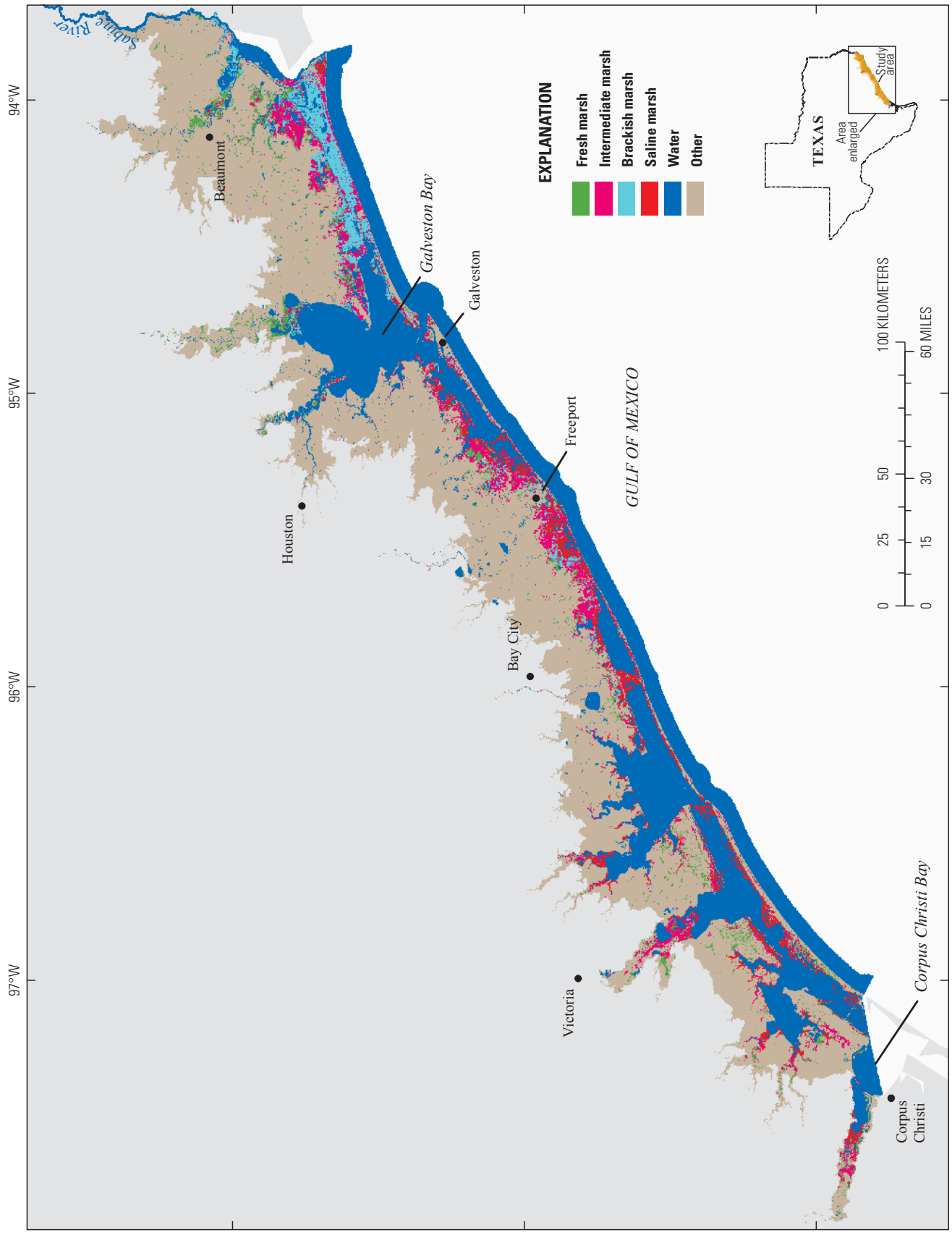

Figure 4. Four-marsh-type classification (fresh, intermediate, brackish, and saline), middle to upper Texas coast, 2010.

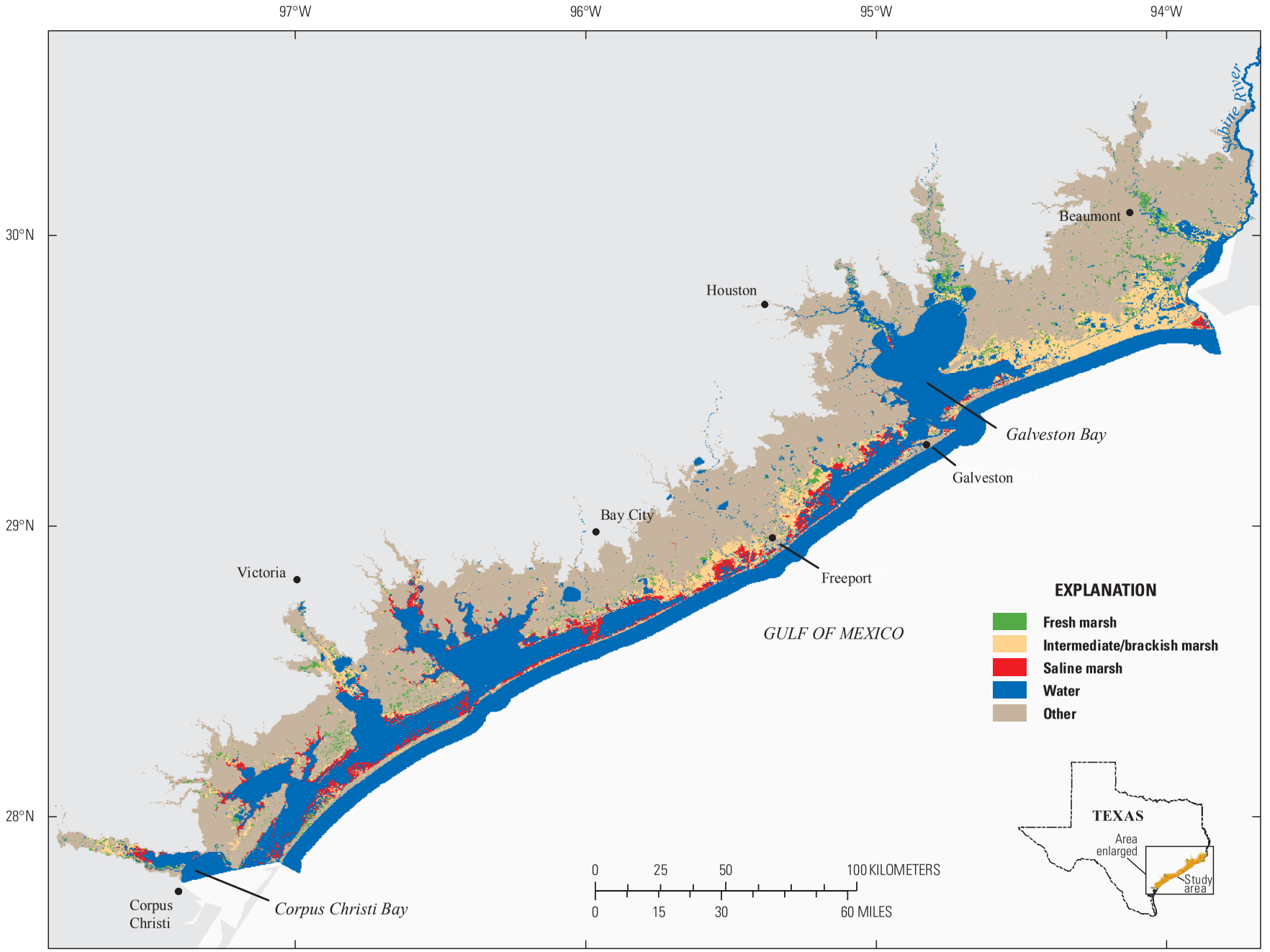

Figure 5. Three-marsh-type classification (fresh, intermediate/brackish, and saline), middle to upper Texas coast, 2010.

classification was better than random classification. Fresh and saline marsh remained relatively unchanged from the four-marsh-type classification (table 4). The combined intermediate/brackish marsh class had a user's accuracy of 74.2 percent (95 percent CI: 71.1–77.3) and a producer's accuracy corrected for bias of 68.2 percent (95 percent CI: 64.4–72). For all marsh vegetation classes in the three-marsh-type classification, mean user's accuracy was 75.6 percent, and mean producer's accuracy corrected for bias was 65.1 percent.

The most dominant classified marsh type was intermediate marsh (table 4), which occurred north of the Gulf Intracoastal Waterway in the Texas Chenier Plain and throughout the Texas Mid-Coast. Saline marsh was the next most dominant marsh, with the highest concentration located in the Texas Mid-Coast and in smaller and more localized areas in the Texas Chenier Plain (fig. 4). Extensive brackish marsh covered much of the coastal areas in the Texas Chenier Plain south of the Gulf Intracoastal Waterway. As expected, fresh marsh was often found farthest inland and upstream in estuaries.

Discussion

This study provided a more objective and repeatable method for classifying marsh types of the middle and upper Texas coast at an extent and greater level of detail than previously available. The seamless classification produced through this work can enable State agencies, including the Texas Parks and Wildlife Department, and landscape-scale conservation partnerships, such as the GCP LCC and the GCJV, to develop and (or) refine conservation plans targeting priority natural resources for marsh-reliant wildlife. Moreover, these data may improve projections of landscape change and serve as a baseline for monitoring future changes resulting from chronic and episodic stressors, including tropical storms, subsidence, sea-level rise, and changes in freshwater flows into Texas bays and marshes (Sasser and others, 2008; Wozniak and others, 2012; Williams, 2013).

Plate 1 depicts marsh vegetation zones representative of prevailing salinity patterns along the Texas coast during 2009–2011. The classification is dated 2010 because it is the mid-point of the multitemporal satellite-based imagery (2009–11) used in this study and the date of the high-resolution airborne imagery that was used to develop image objects. Most of Texas underwent an extreme drought in 2011, which impacted freshwater inflow and salinity conditions in estuaries of coastal Texas (C. Schoenbaechler, C. Guthrie, T. McEwen, and S. Negusse, Texas Water Development Board, written commun., 2013). For estuaries in the study area, the 2011 drought led to an overall decrease in annual freshwater inflow of approximately 32,687 cubic hectometers (hm^3) from historical mean annual inflow, resulting in a mean salinity during 2011 that was 65.6 percent higher than historical means (C. Schoenbaechler, C. Guthrie, T. McEwen, and S. Negusse, Texas Water Development Board, written commun., 2013). Although the classification is dated 2010, this classification does not depict salinity or vegetation conditions for a single date, nor does it necessarily project vegetation conditions for extended periods into the future. Composition and distribution of vegetation communities along the coast are dynamic and influenced strongly by frequency and duration of flooding, salinity, acute disturbances, and other factors; thus, marsh zonation documented during this project is likely to vary temporally and spatially in response to changes in these key controlling factors. Consequently, consideration should be given to repeating this survey on a relatively fixed frequency (every 5 years), similar to the schedule of marsh vegetation survey and classification in Louisiana (Sasser and others, 2008) and other landscape scale mapping efforts such as NLCD and C-CAP. The most appropriate use of this and future classification is for understanding general distribution and overall changes in areal coverage of marshes at the landscape level.

Lessons learned in this classification could be applied to future classifications, particularly because it relates sample design, data preprocessing (using Landsat Climate Data Record [CDR] imagery, if available), extending the classification to include south Texas, exploring spectral separability (Jeffries-Matusita distance; Schmidt and Skimore, 2003) of marsh types, using fewer but more targeted image dates, and utilizing newly available data and technology. Each of these factors are discussed in more detail in the following paragraphs.

Few fresh marsh ground reference data were collected throughout the study area, and ground reference points for brackish marsh were rare in Path 26 Row 41, which likely contributed to low classification rates for fresh marsh in that area. In comparison to the Louisiana coastal zone, marshes in the Texas coastal zone occur within a much narrower transitional gradient between uplands and open waters of the Gulf of Mexico. The narrow transitional gradient in Texas coastal marshes, combined with limited prior knowledge of the distribution of marsh types in the study area, likely contributed to our inability to obtain equal numbers of reference points for all marsh types. Additionally, this classification was based on approximately 1,000 ground reference locations, whereas the Louisiana marsh classification is usually informed by more than 8,300 reference locations (Sasser and others, 2014). For Texas, more than 3,041.7 km^2 of marsh (that is, all marsh types) were mapped with a sampling density for all helicopter and supplemental marsh locations from TPWD (excluding supplemental palustrine emergent marsh from NWI, water, and "other" locations [helicopter observations and in-place observations by TPWD]) of one reference location for every 4.1 km^2 of mapped marsh. Sampling density by marsh type was as follows: (1) one observation of fresh marsh per 20.3 km^2 mapped, (2) one observation of intermediate marsh per 4.3 km^2 mapped, (3) one observation of brackish marsh per 3.6 km^2 mapped, and (4) one observation of saline marsh per 3.3 km^2 mapped. By comparison, more than 14,652.3 km^2

of marsh in Louisiana were mapped, with an overall sampling density of one reference location for every 3.5 km^2 of mapped marsh. Sampling density for each specific marsh type in Louisiana was similar for all marsh types with one observation per an estimated 2.4 km^2 mapped. These sample densities apply to the entire study area; however, DTs were developed for each TM scene (fig. 1). Future classifications of Texas coastal marsh could seek a sample design that ensures that reference locations are distributed among all marsh types within each Landsat TM scene and that the number of reference points within each marsh type are proportional to their areal coverage.

For the four-marsh-type classification, intermediate marsh had the lowest accuracy, with both producer's and user's accuracy below 50 percent. Classification of intermediate marsh is uncommon outside the Gulf Coast, likely because it is rare or defined as "tidal freshwater marsh" in other regions (Nyman and Chabreck, 2012). This fact, combined with the spectral similarities of intermediate marsh to other marsh types, likely contributed to its low classification accuracy. It may be valuable to assess spectral separability (Jeffries-Matusita distance) of dominant marsh vegetation species within each type prior to future classifications. Because of the relatively narrow marsh zonation in Texas as compared to that in Louisiana, there may be utility in using an alternative classification scheme of three marsh types in which intermediate and brackish marsh are combined. Application of this alternative classification should be restricted to those areas where delineation of four marsh zones is not essential.

The feasibility of incorporating atmospheric correction could be investigated; however, Huang and others (2002) suggested that the use of tasseled cap transformation based on TOA reflectance is appropriate for regional applications in which atmospheric correction may not be feasible. Additionally, extensive mapping efforts, such as NLCD, utilize imagery that is corrected for TOA reflectance units (Xian and others, 2009). Landsat surface reflectance CDR provides surface reflectance for Landsat TM, ETM+, and various indices for download (http://landsat.usgs.gov/CDR_ECV.php). If available, the utility of Landsat CDR imagery could be explored when updating this classification.

This classification was not applied to areas south of Corpus Christi Bay, primarily because they contain relatively little emergent marsh. Nevertheless, mapping of areas south of Corpus Christi Bay could be considered in future classifications to depict emergent marsh types along the entire Texas coast, thereby enabling comprehensive and consistent planning for all emergent marsh habitats in Texas (Texas Coastal and Estuarine Land Conservation Program, unpub. data, 2010).

Obtaining cloud-free imagery along the Gulf Coast is often difficult. Future studies could explore the possibility of using a more targeted image date selection by analyzing phenological differences and spectral separability (Jeffies-Matusita distance) of marsh vegetation classes by using 30-m TOA NDVI from Web-enabled Landsat data (WELD; Brown and others, 2006; Roy and others, 2010; Kovalskyy and others, 2012). Future classifications could also ensure that spatial registration between the existing classifications is sufficient prior to any change detection analyses. Additionally, because of the cost of helicopter surveys, a methodology similar to NOAA C-CAP and the NLCD efforts could be explored (Xian and others, 2009). These methods include utilizing change detection to identify changed areas and focusing ground reference data collection and reclassification only on areas that have undergone change. These approaches may help guide ways to enhance both performance and efficiency of future classifications.

Additionally, as technology continues to advance and new data become available, it is pertinent that these data are tested and utilized, with particular consideration given to synoptic hyperspectral remote sensing data and lidar-based vegetation metrics, including vegetation height and structure. Synoptic hyperspectral remote sensing data could provide added spectral resolution for improving the delineation of marsh vegetation communities, perhaps extending classification specificity to the species level (Best and others, 1981; Penuelas and others, 1993; Schmidt and others, 2004; Rosso and others, 2005; Yang and others, 2009). Lidar data metrics such as vegetation height or texture could help improve the delineation of marsh vegetation communities. Although vegetation height does tend to vary among marsh plant species, the detectability of variation within marsh vegetation communities could be explored. Because coastal vegetation is very dynamic, especially when subject to hurricane-related impacts, the lidar acquisition date is particularly important. At the time of this classification, lidar data available for the Texas coast was captured in 2006. Because of the possible residual effects of Hurricane Rita in 2005 and Hurricane Ike in 2008, only bare-earth elevations were used in this study. One way to alleviate these issues is by using the best data available per Landsat TM footprint.

References Cited

Best, R., Wehde, M., and Linder, R., 1981, Spectral reflectance of hydrophytes: Remote Sensing of Environment, v. 11, p. 27–35.

Boryan, C., Yang, Z., Di, L., and Mueller, R., 2011, Monitoring US agriculture, National Agricultural Statistics Service Cropland Data Layer Program: Geocarto International, v. 26, p. 341–358.

Brown, M.E., Pinzón, J.E., Didan, K., Moriette, J.T., and Tucker, C.J., 2006, Evaluation of the consistency of long-term NDVI time series derived from AVHRR, SPOT-Vegetation, SeaWiFS, MODIS and Landsat ETM+ Sensors: IEEE Transactions on Geoscience and Remote Sensing, v. 44, p. 1787.

Chabreck, R.H., 1972, Vegetation, water and soil characteristics of the Louisiana coastal marshes: Baton Rouge, Louisiana State University, Louisiana Agricultural Experiment Station, Bulletin 664.

Chabreck, R.H., and Linscombe, G., 1978, Vegetative type map of the Louisiana coastal marshes: Baton Rouge, Louisiana Department of Wildlife and Fisheries.

Chabreck, R.H., and Linscombe, G., 1988, Vegetative type map of the Louisiana coastal marshes: Baton Rouge, Louisiana Department of Wildlife and Fisheries, set of 10 maps.

Chabreck, R.H., and Linscombe, G., 1997, Vegetative type map of the Louisiana coastal marshes: Baton Rouge, Louisiana Department of Wildlife and Fisheries.

Chabreck, R., and Linscombe, G., 2001, Vegetative type map of the Louisiana coastal marshes: New Orleans, Louisiana Department of Wildlife and Fisheries.

Chabreck, R.H., Palmisano, A.W., Jr., and Joanen, T., 1968, Vegetative type map of the Louisiana coastal marshes: Baton Rouge, La., Louisiana Department of Wildlife and Fisheries.

Congalton, R.G., and Green, K., 2009, Assessing the accuracy of remotely sensed data principles and practices (2d ed.): Boca Raton, Fla., CRC Press, 183 p.

Couvillion, B.R., and Beck, H., 2013, Marsh collapse thresholds for coastal Louisiana estimated using elevation and vegetation index data, *in* Brock, J.C., Barras, J.A., and Williams, S.J., eds., Understanding and predicting change in the coastal ecosystems of the northern Gulf of Mexico: Coconut Creek, Fla., Journal of Coastal Research, Special Issue no. 63, 262 p.

Crist, E.P., and Cicone, R.C., 1984, A physically-based transformation of Thematic Mapper data—The TM tasseled cap: IEEE Transactions on GeoScience and Remote Sensing, v. 22, p. 256–263.

Finkbeiner, M., Robinson, C., Simons, J.D., Summers, A., Wood, J., and Lopez, C., 2009, Atlas of shallow-water benthic habitats of coastal Texas—Espiritu Santo Bay to Lower Laguna Madre, 2004 and 2007: Charleston, S.C., National Oceanic and Atmospheric Administration Coastal Services Center, 60 p.

Glick, P., Clough, J., Polaczyk, A., Couvillion, B., and Nunley, B., 2013, Potential effects of sea-level rise on coastal wetlands in southeastern Louisiana, *in* Brock, J.C., Barras, J.A., and Williams, S.J., eds., Understanding and predicting change in the coastal ecosystems of the northern Gulf of Mexico: Coconut Creek, Fla., Journal of Coastal Research, Special Issue no. 63, 262 p.

Gosselink, J.G., Cordes, C.L., and Parsons, J.W., 1979, An ecological characterization study of the Chenier Plain coastal ecosystem of Louisiana and Texas (v. 1–3): U.S. Fish and Wildlife Service, Office of Biological Services, FWS/OBS 78/09–78/11.

Hill, M.O., 1979, Twinspan—A FORTRAN program for arranging multivariate data in an ordered two-way table by classification of the individuals and attributes: Ithaca, N.Y., Cornell University Press.

Homer, C., Dewitz, J., Fry, J., Coan, M., Hossain, N., Larson, C., Herold, N., McKerrow, A., VanDriel, J.N., and Wickham, J., 2007, Completion of the 2001 National Land Cover Database for the conterminous United States: Photogrammetric Engineering and Remote Sensing, v. 73, p. 337–341.

Huang, C., Yang, W.L., Homer, C., and Zylstra, G., 2002, Derivation of a tasseled cap transformation based on Landsat 7 at-satellite reflectance: International Journal of Remote Sensing, v. 23, p. 1741–1748.

Johnson, J.S., Cairns, D.M., and Houser, C., 2013, Coastal marsh vegetation assemblages of Galveston Bay—Insights for the East Texas Chenier Plain: Wetlands, v. 33, p. 861–870.

Kovalskyy, V., Roy, D.P., and Zhang, X.Y., 2012, The suitability of multi-temporal Web-enabled Landsat data NDVI for phenological monitoring—A comparison with flux tower and MODIS NDVI: Remote Sensing Letters, v. 3, p. 325–334.

Marcy, D., Brooks, W., Draganov, K., Hadley, B., Haynes, C., Herold, N., McCombs, J., Pendelton, M., Ryan, S., Schmid, K., Sutherland, M., and Waters, K., 2011, New mapping tool and techniques for visualizing sea level rise and coastal flooding impacts, *in* Wallendorf, L.A., Jones, C., Ewing, L., and Battalio, B., eds., 2011 Solutions to Coastal Disasters Conference, Anchorage, Alaska, June 26–June 29, 2011, Proceedings: Reston, Va., American Society of Civil Engineers, 954 p.

Mitchell, M.K., Ballard, B.M., Visser, J.M., Brasher, M.G., and Redeker, E.J., in press, Delineation of coastal marsh types along the central Texas coast: Wetlands.

Moore, I.D., Grayson, R.B., and Ladson, A.R., 1991, Digital terrain modelling—A review of hydrological, geomorphological and biological applications: Hydrological Processes, v. 5, p. 3–30.

Nyman, J.A., and Chabreck, R.H., 2012, Managing coastal wetlands for wildlife—The wildlife techniques manual, *in* Silvy, N.J., ed., Management: Baltimore, Md., The Johns Hopkins University Press, v. 2, 414 p.

O'Neil, T., 1949, The muskrat in the Louisiana coastal marsh: New Orleans, Louisiana Department of Wildlife and Fisheries.

Osland, M.J., Enwright, N., and Stagg, C.L, in press, Freshwater availability and coastal wetland foundation species—Ecological transitions along a rainfall gradient: Ecology.

Parker, B., Hess, K.W., Milbert, D.G., and Gill, S., 2003, National VDatum—The implementation of a national vertical datum transformation database: U.S. Hydrographic Conference, Biloxi, Miss., accessed January 15, 2013, at http://vdatum.noaa.gov/download/publications/2003_parker_USHydro_nationalvdatum.pdf.

Penuelas, J., Filella, I., Biel, C., Serrano, L., and Save, R., 1993, The reflectance at the 950–970 nm region as an indicator of plant water status: International Journal of Remote Sensing, v. 14, p. 2593–2610.

Prism Climate Group, 2012, United States average annual precipitation, 1981–2010 (800 m; BIL): PRISM Climate Group at Oregon State University, accessed March 14, 2014, at http://www.prism.oregonstate.edu/inc/images/graphics/normals/800m/ppt/viewable/PRISM_ppt_30yr_normal_800mM2_annual.png?ts=2014319.

Rosso, P.H., Ustin, S.L., and Hastings, A., 2005, Mapping marshland vegetation of San Francisco Bay, California, using hyperspectral data: International Journal of Remote Sensing, v. 26, p. 5169–5191.

Rouse, J.W., Haas, R.H., Schell, J.A., and Deering, D.W., 1974, Monitoring Vegetation Systems in the Great Plains with ERTS, *in* the Third Earth Resources Technology Satellite-1 Symposium, Greenbelt, Md., 1973, Proceedings: Greenbelt, Md., NASA SP–351, p. 3010–3017.

Roy, D.P., Ju, J., Kline, K., Scaramuzza, P.L., Kovalskyy, V., Hansen, M.C., Loveland, T.R., Vermote, E.F., Zhang, C., 2010, Web-enabled Landsat data (WELD)—Landsat ETM+ composited mosaics of the conterminous United States: Remote Sensing of Environment, v. 114, p. 35–49.

Sasser, C.E., Visser, J.M., Mouton, E., Linscombe, J., and Hartley, S.B., 2008, Vegetation types in coastal Louisiana in 2007: U.S. Geological Survey Open-File Report 2008–1224, 1 sheet, scale 1:550,000.

Sasser, C.E., Visser, J.M., Mouton, E., Linscombe, J., and Hartley, S.B., 2014, Vegetation types in coastal Louisiana in 2013: U.S. Geological Survey Scientific Investigations Map 3290, 1 sheet, scale 1:550,000.

Schmidt, K.S., and Skidmore, A.K., 2003, Spectral discrimination of vegetation types in a coastal wetland: Remote Sensing of Environment, v. 85, p. 92–108.

Schmidt, K.S., Skidmore, A.K., Kloosterman, E.H., Oosten, H., van, Kumar, L., and Janssen, J.A.M., 2004, Mapping coastal vegetation using an expert system and hyperspectral imagery: Photogrammetric Engineering and Remote Sensing, v. 70, p. 703–715.

Tiner, R.W., 1993, Field guide to coastal wetland plants of the southeastern United States: Amherst, Mass., The University of Massachusetts Press, 328 p.

U.S. Geological Survey Earth Resources Observation and Science Center (EROS), 2003, Topographic science project—Elevation Derivatives for National Applications (EDNA) Compound Topographic Index (CTI): Sioux Falls, S. Dak., U.S. Geological Survey EROS.

Visser, J.M., Sasser, C.E., Chabreck, R.H., and Linscombe, R.G., 1998, Marsh vegetation types of the Mississippi River Deltaic Plain: Estuaries, v. 21, p. 818–828.

Visser, J.M., Sasser, C.E., Linscombe, R.G., and Chabreck, R.H., 2000, Marsh vegetation types of the Chenier Plain, Louisiana, USA: Estuaries, v. 23, p. 318–327.

Williams, S.J., 2013, Sea-level rise implications for coastal regions, *in* Brock, J.C., Barras, J.A., and Williams, S.J., eds., Understanding and predicting change in the coastal ecosystems of the Northern Gulf of Mexico: Coconut Creek, Fla., Journal of Coastal Research, Special Issue no. 63, 262 p.

Wilson, B.C., and Esslinger, C.G., 2002, North American Waterfowl Management Plan, Gulf Coast Joint Venture—Texas Mid-Coast Initiative: Albuquerque, N. Mex., North American Waterfowl Management Plan, 28 p.

Wozniak, J.R., Swannack, T.M., Butzler, R., Llewellyn, C., and Davis, S.E. III, 2012, River inflow, estuarine salinity, and Carolina wolfberry fruit abundance—Linking abiotic drivers to whooping crane food: Journal of Coastal Conservation, v. 16, p. 345–354.

Xian, G., Homer, C., and Fry, J., 2009, Updating the 2001 National Land Cover Database land cover classification to 2006 by using Landsat imagery change detection methods: Remote Sensing of Environment, v. 113, p. 1133–1147.

Xu, H., 2006, Modification of normalized difference water index (NDWI) to enhance open water features in remote sensed imagery: International Journal of Remote Sensing, v. 27, p. 3025–3033.

Xu, J., Myers, E., Jeong, I., and White, S., 2013, VDatum for coastal waters of Texas and western Louisiana—Tidal datums and topography of the sea surface: NOAA Technical Memorandum NOS CS–27.

Yang, C., Everitt, J.H., Fletcher, R.S., Jensen, R.R., and Mausel, P.W., 2009, Evaluating AISA+ hyperspectral imagery for mapping black mangrove along the south Texas Gulf Coast: Photogrammetric Engineering and Remote Sensing, v. 75, p. 425–435.

Publishing support provided by
Lafayette Publishing Service Center

ISSN 2328-0328 (online)
http://dx.doi.org/10.3133/sir20145110